*Synthesis and Reactivity in Inorganic, Metal-Organic, and Nano-Metal Chemistry*, 42:1064–1070, 2012

ISSN: 1553-3174 print / 1553-3182 online
DOI: 10.1080/15533174.2011.652279

Taylor & Francis
Taylor & Francis Group

# Chemical *In Situ* Polymerization of Polypyrrole Nanoparticles on the Hydrophilic/Hydrophobic Surface of $SiO_2$ Substrates

**Jian-Sheng Wu, Da-Wei Gu, Da Huang, and Lin-Jiang Shen**
*College of Science, Nanjing University of Technology, Nanjing, P. R., China*



**Polypyrrole (PPy) nanoparticles formed by chemical *in situ* polymerization were deposited on the hydrophilic/hydrophobic surface of $SiO_2$ substrates to give the diversely morphology, respectively. The morphologies of PPy nanoparticles deposit were investigated using optical microscope, scanning electron microscope (SEM), and atomic force microscope (AFM) imaging techniques. The morphology of Y- and T-shape wrinkles was observed on the hydrophilic surface of $SiO_2$ substrate, while the morphology of polygon-shape wrinkles on the hydrophobic surface of $SiO_2$ substrate, and this distinction is due to the difference of the surface energy between the hydrophilic and hydrophobic surface of $SiO_2$ substrate and so-called "memory effect."**

**Keywords** hydrophilic/hydrophobic surface, *in situ* polymerization, nanoparticle, polypyrrole

## INTRODUCTION

Conducting polymers (CPs) have attracted great interest in recent decades due to their combination of useful mechanical, optical, and electronic properties.[1–4] In particular, polypyrrole (PPy), one of the most widely studied CPs, is excellent for construction of nanostructural and device design because of the chemical stability, electrical, electronic, and optical properties similar to some metals or semiconductors while keeping flexibility, ease of processing, and modifiable electrical conductivity.[4–7] Since the polypyrrole nanoparticle and nanotube are well applicable for nanocomposite and nanocarbon precursor,[8–10] PPy becomes one of the most potential candidates for many applications.

Electrochemical polymerization, as a means for preparing many conducting polymers, has been studied for years. It was reported that PPy could be deposited by such way on a wide range of conducting anodes, such as noble metal coated with base metals, graphite, glassy carbon, and also on commodity metals under certain conditions. The observation of the morphology, however, showed that there were a great many wrinkles laid over the surface, which is heavily dependent on the characteristics of the anode, as well as on the experimental variables. The further study confirmed that the wrinkles affected on the mechanical strength and electrical properties of the PPy film.[11,12] As a result, challenges still exist in the aspects of the origin of the wrinkle morphology and mechanism for the nanoparticles deposition and film growth even though they have been well studied for years.[13,14]

Chemical *in situ* polymerization of PPy has the characters of easy preparation and suitable for mass production in comparison with the electrochemical method.[3,4] We used the approach of chemical *in situ* polymerization to prepare PPy nanoparticles and further deposit the PPy nanoparticles on different hydrophilic/hydrophobic surface of $SiO_2$ substrates to form the thin films. The morphologies of nanoparticles deposition film were investigated using optical microscopy, scanning electron microscopy (SEM), and atomic force microscopy (AFM) techniques, respectively.

## EXPERIMENTAL

### Chemicals and Reagents

Pyrrole (Sigma-Aldrich, USA, 98%), octadecyltrichlorosilane (OTC, Sigma-Aldrich, USA, 90%), and $FeCl_3 \cdot 6H_2O$ (AR) were purchased from commercial sources and used directly without further purification. All other reagents were analytically pure. Water used throughout was deionized and then double distilled. $SiO_2$ glass substrates used in the experiments were purchased from commercial sources of quartz slide with the sizes of ~0.9 cm × 2.5 cm × 0.1 cm.

### Preparation of Hydrophilic/Hydrophobic $SiO_2$ Glass Substrate

After immersing the $SiO_2$ substrates into chromic acid mixture for more than 24 h, the clean $SiO_2$ substrates were obtained by ultrasonically washing with water for more than three times. The hydrophilic $SiO_2$ substrates were made by immersing the clean $SiO_2$ substrates in a freshly prepared "Piranha solution" (a

Received 19 August 2011; accepted 1 November 2011.
The authors thank the National Nature Science Foundation of China for financial support (Grant No.: 10774076).
Address correspondence to Lin-Jiang Shen, College of Science, Nanjing University of Technology, Nanjing, P. R. China. E-mail: ljshen@njut.edu.cn

mixture of 98% $H_2SO_4$, and 30% $H_2O_2$, 7:3, v/v) at ~70°C for ~2 h, rinsed thoroughly with plenty of water, and finally dried at room temperature in a dust-free vacuum oven for 1 h.[15] The hydrophobic $SiO_2$ glass substrates were made from hydrophilic substrates by placed the former in a flask charged with a toluene solution (20 mL) of octadecyltrichlorosilane (0.2 mL), and the solution was refluxed for 2 h. Upon cooling to room temperature, the substrates were removed from the flask, successively washed with copious amounts of toluene and ethanol, and then dried at room temperature in a dust-free vacuum oven for 1 h.[15]

### Deposition of PPy Nanoparticles on $SiO_2$ Glass Substrates

To prepare the reaction solution, equal volumes of an aqueous solution 0.2 M in pyrrole and an aqueous solution 0.46 M in ferric chloride were mixed in an ice bath. The cleaned $SiO_2$ substrates covered with a thin adhesive tape on one side were immersed into the reaction solution vertically. After the reaction, the $SiO_2$ substrates were removed off and washed by distilled water three times and dried in vacuum at room temperature.

### Physical Measurements

Contact angles of the $SiO_2$ substrates were measured on a dataphysics OCA20 contact-angle system at ambient temperature. The optical microscopy experiments were performed with a Caikang XPR500D optical microscope (Shanghai, China). Morphological examination was conducted using a Jeol JSM-5900 scanning electron microscope (Tokyo, Japan). Studies involving AFM imaging were carried out in noncontact mode in air at room temperature using a Benyuan CSPM5000 scanning probe microscope (Beijing, China).

## RESULTS AND DISCUSSION

### Characterization of Surface of $SiO_2$ Substrates

Contact angles at ambient temperature of the surfaces of (a) clean, (b) hydrophilic, and (c) hydrophobic $SiO_2$ substrates to water were measured and the experimental results are shown in Figure 1. It is clearly revealed that the static contact angle decreased significantly from 52.3 ± 0.5° to 24.8 ± 0.5° after treatment for substrates with the piranha solution. Further treatment with OTC resulted in a sharp increase in the data (93.6 ± 0.5°), indicating that the wettability of the surface has reversed. Generally, the wettability is associated with the surface energy of the substrate. To obtain the surface energy of the substrates, the Owens method was used. By measuring the contact angles of the ethylene glycol on the hydrophilic/hydrophobic substrates at room temperature further, the surface energy for the substrates of $SiO_2$ can be obtained. The experimental result of the surface energy for the hydrophilic surface of $SiO_2$ substrate is 83.8 mN/m, and 32.2 mN/m for the hydrophobic surface. These results are consistent with the expectation from the chemical composition of the surface.

### Optical Microscopy Study of PPy Nanoparticles Deposited on $SiO_2$ Substrates

Optical microscopy image is a simple but convenient method for large-scale initial observation. Optical microscopy photographs for the deposition of PPy nanoparticles on various surfaces of $SiO_2$ substrates under different reaction time are illustrated in Figure 2. It can be found that the Y- and T-shaped wrinkle morphology appeared on both hydrophilic and hydrophobic surfaces of $SiO_2$ substrates as the reaction continuing to 2 h. Then, the wrinkle morphology spread on the whole surfaces of $SiO_2$ substrates during the following reaction time (i.e., 3 or 4 h). In this period, the size of wrinkles increased significantly after the reaction time further reaching to 6 h. Though the wrinkle on both of the hydrophilic and hydrophobic surfaces of $SiO_2$ substrates exhibited Y- and T-shaped morphology as before, a distinct difference can be found. For hydrophilic substrate the wrinkles morphology tended to in an open morphology, while a closed polygon shape on the hydrophobic surface. In addition, such Y- and T-shaped wrinkle morphology is quite similar with the observation of PPy deposition on the surface of ITO using electrochemical polymerization by Miles and coworkers.[14]

### SEM Study of PPy Nanoparticles Deposited on $SiO_2$ Substrates

Because of the limited magnification of the optical microscopy images, further research using SEM as a supplement method was carried out to get the detailed information of the wrinkles morphology. The SEM photo for the sample of PPy deposition on the hydrophilic substrate under the reaction time of 2 h is displayed in Figure 3, which showed obviously the PPy nanoparticles spread on hydrophilic surface of $SiO_2$ substrate. Meanwhile, the Y- and T-shaped wrinkles morphology appeared. From the enlarged photo (Figure 3), it can be found that the dimension of mountain-like wrinkle morphology was about 10–20 $\mu$m in length, and less than 1 $\mu$m in width. It is necessary to point out, that the size of PPy particles

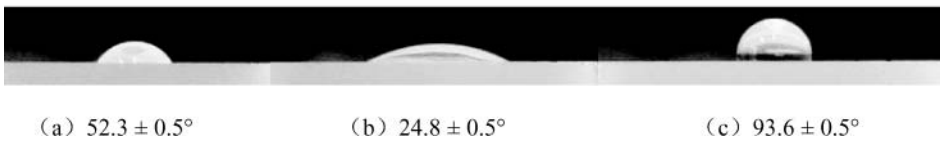


FIG. 1. Static contact angles ($\theta$) of various $SiO_2$ substrate surfaces and water: (a) the original clean $SiO_2$ glass substrate; (b) hydrophilic $SiO_2$ glass substrate; (c) hydrophobic $SiO_2$ glass substrate.

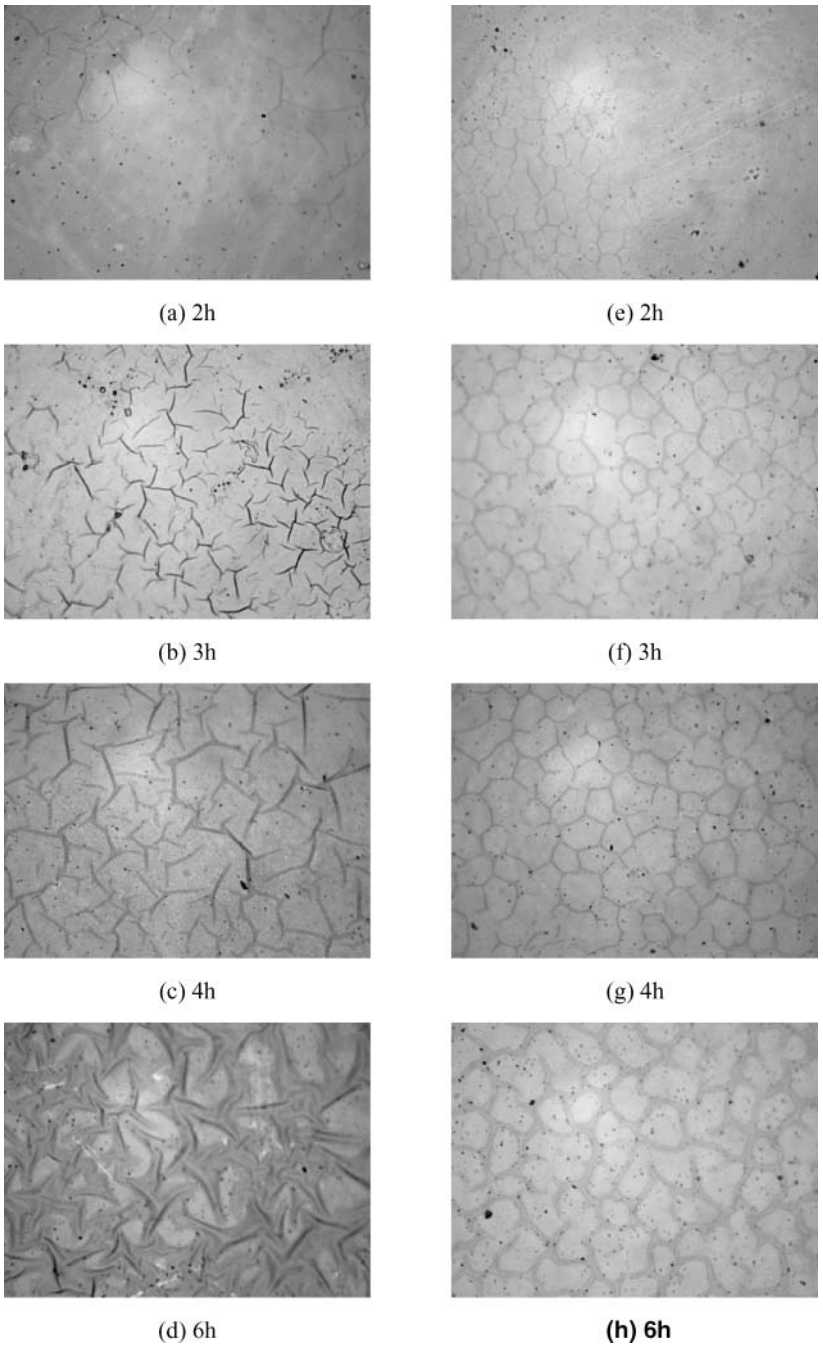


FIG. 2. The optical microscope micrographs for the depositon of PPy under reaction time of 2, 3, 4, and 6 h for the hydrophilic surface of $SiO_2$ substrate (a, b, c, and d) the hydrophobic surface of $SiO_2$ substrate (e, f, g, and h).

seems about 100 nm according to the AFM images shown subsequently, much less than the dimension of the wrinkle morphology.

### AFM Study of PPy Nanoparticles Deposited on $SiO_2$ Substrates

This set of experiments included samples of PPy deposits produced in *ex situ* experiments at various advanced reaction times (greater than 1 h) corresponding to relatively thick films and then subjected to AFM examination. Out of a large number of runs performed we have chosen to describe a few selected examples of typical films. PPy deposits morphology with an area of $40 \times 40$ $\mu$m as well as the cross-section image labeled are demonstrated in Figure 4, indicating that the mountain-like wrinkles were quite uniform, with the height of $\sim$180 nm and the width of $\sim$950 nm, respectively.

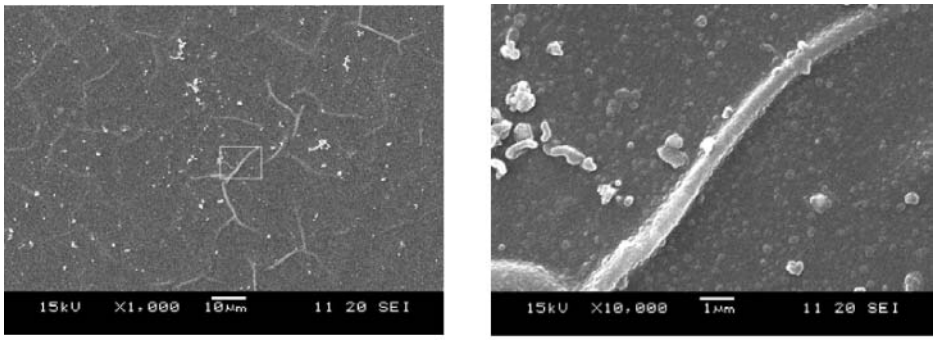


(a) (b)

FIG. 3. (a) The SEM micrograph of PPy nanoparticles deposition on the hydrophilic surface of $SiO_2$ substrate under the reaction time of 2 h; (b) the magnified image corresponding to the rectangle in (a).



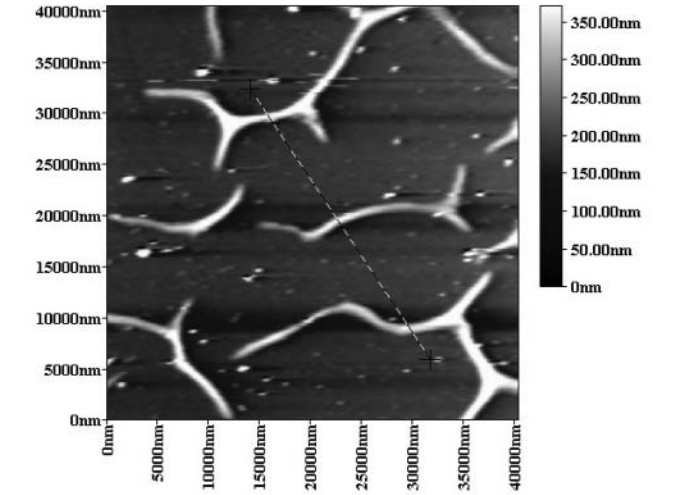


(a)

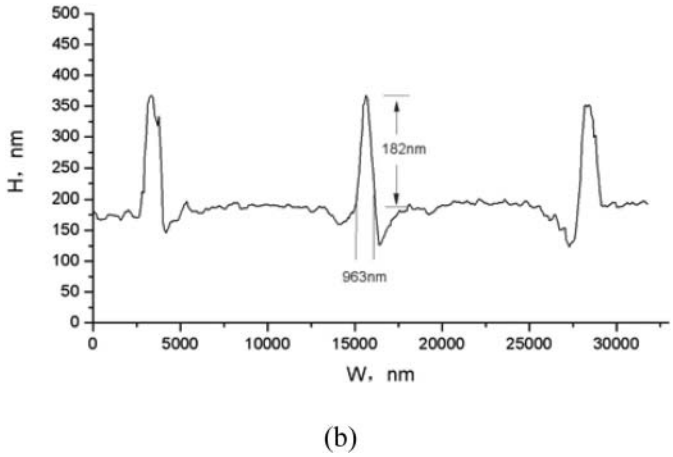


(b)

FIG. 4. (a) The AFM image of PPy deposits morphology with an area of $40 \times 40$ $\mu$m and (b) the cross-section image.

AFM images of PPy deposits on hydrophilic versus hydrophobic surface of $SiO_2$ substrates under different advanced reaction times (1, 2, 3, 4, and 6 h) are shown in Figure 5. PPy nanoparticles deposited and could be formed a thin film on the hydrophilic and hydrophobic surfaces of $SiO_2$ substrates when the reaction time was 1 h. In the case of such relate short reaction period, however, it is obvious that the morphology of film on both substrates is different. For hydrophilic substrate, the nanoparticle diameter and the film thickness are ∼60 nm and 20–30 nm respectively, apparently larger than those on hydrophobic substrate (∼20 nm in diameter and ∼16 nm in thickness). The pattern of the film on hydrophilic substrate seems more incompact as comparing with that on hydrophobic substrate. The dependence of the film morphology on the substrate is mainly due to the reverse surface energy of the hydrophilic and hydrophobic substrates.

When the reaction time reaches to 2 h, uniform and close films were observed in the hydrophilic and hydrophobic surfaces of $SiO_2$ substrates, whereas different growing rate was observed with the film thickness of ∼60 nm in the former versus ∼40 nm in the latter. Besides, it was observed that wrinkles morphology started to appear on this stage according to the optical microscopy.

Wrinkles spread on the whole surface of $SiO_2$ substrates when the reaction time reaches to 3 h. Herein an increased scanning area from $4 \times 4$ $\mu$m to $80 \times 80$ $\mu$m was performed to have a deeper view of the overall film morphology because of the necessary for observation of the large scale of the wrinkles. As shown in Figure 5, there were obvious rod-like and Y- and T- shaped wrinkles, which were coincident with the images observed by optical microscopy. The difference between the two films lies in two aspects: (a) the wrinkles are much larger in both size and amount for the former, and (b) the two films have different thickness, with ∼85 nm in the former versus ∼60 nm in the latter.

The thickness of the films kept on increasing when reaction time reaches to 4 h. The wrinkles became bigger and the

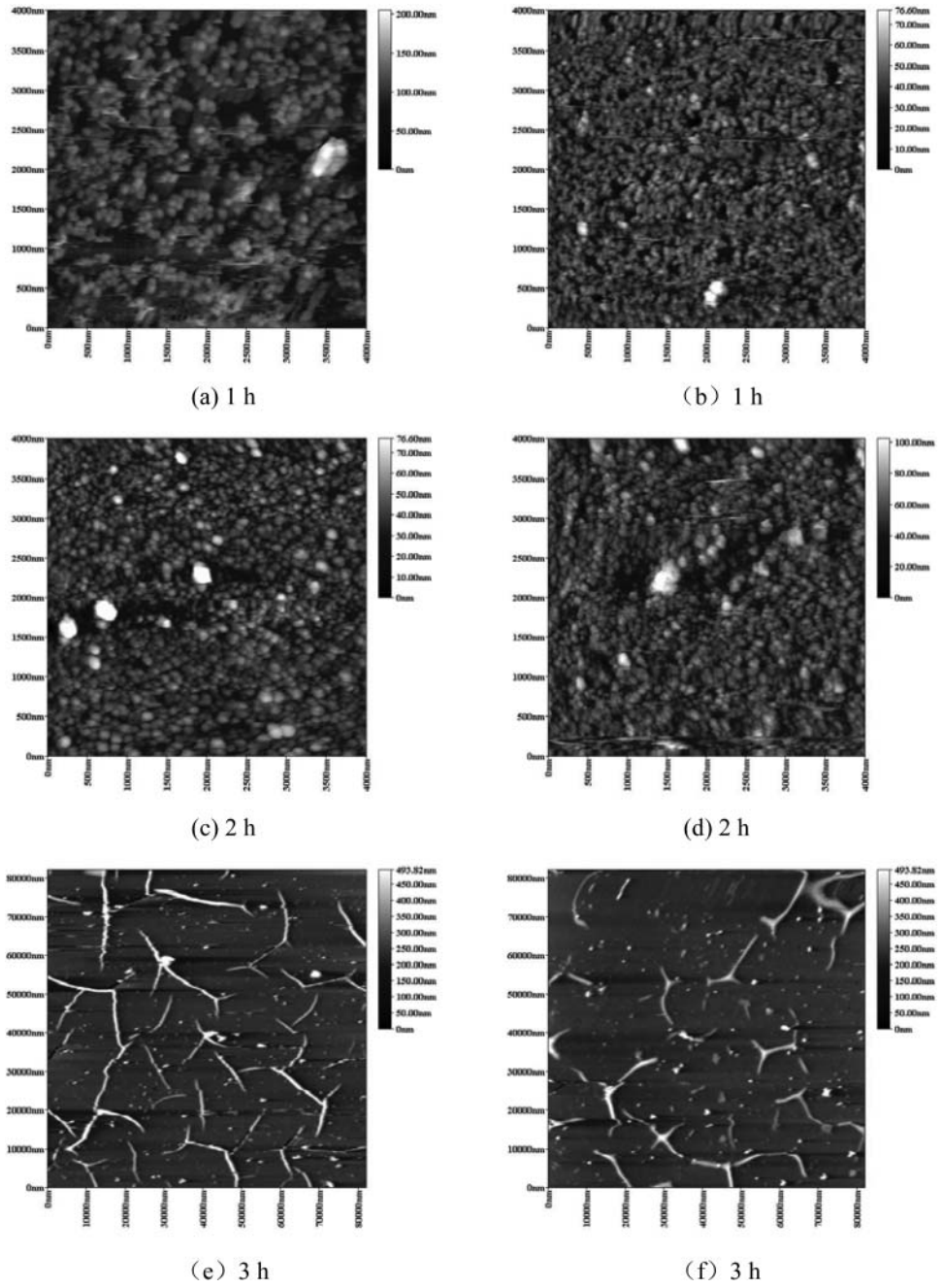


FIG. 5. The AFM images of PPy deposits on the hydrophilic (a, c, e, g, I, and k) versus hydrophobic surfaces of $SiO_2$ substrates (b, d, f, h, j, and l) under different reaction time.

separated Y- and T- shaped wrinkles interconnected to form into even bigger wrinkles. When the reaction time further reached to 6 h, a significant kind of open Y- and T- shaped wrinkles morphology was observed on the hydrophilic surface of the substrate. However, closed polygon–shaped wrinkles were observed on the hydrophobic surface of $SiO_2$ substrate, which was quite coincidence with the morphology observed by optical microscopy.

According to the AFM images as shown previously, the size of the wrinkles (Table 1) and the thickness of the PPy films (Figure 6) under different reaction times can be obtained. In this work the thickness of films were direct obtained by AFM. Three scratch marks were made on each samples of the PPy film by a steel blade, and then scanning cross section was done on each scratch marks. The thickness of the film is determined by the average value from the three scratch marks. From the

TABLE 1
Size of the wrinkles formed on different surfaces of $SiO_2$ substrates

| Reaction time (h) | | 1 | 2 | 3 | 4 | 6 |
|---|---|---|---|---|---|---|
| Hydrophilic | Height (nm) | — | 100 | 200–300 | 500–700 | 800–1000 |
| | Width ($\mu$m) | — | 0.5 | 1–2 | 3–4 | 4–6 |
| Hydrophobic | Height (nm) | — | 50 | 150–200 | 300–400 | 600 |
| | Width ($\mu$m) | — | 0.3 | 1 | 2 | 3–4 |

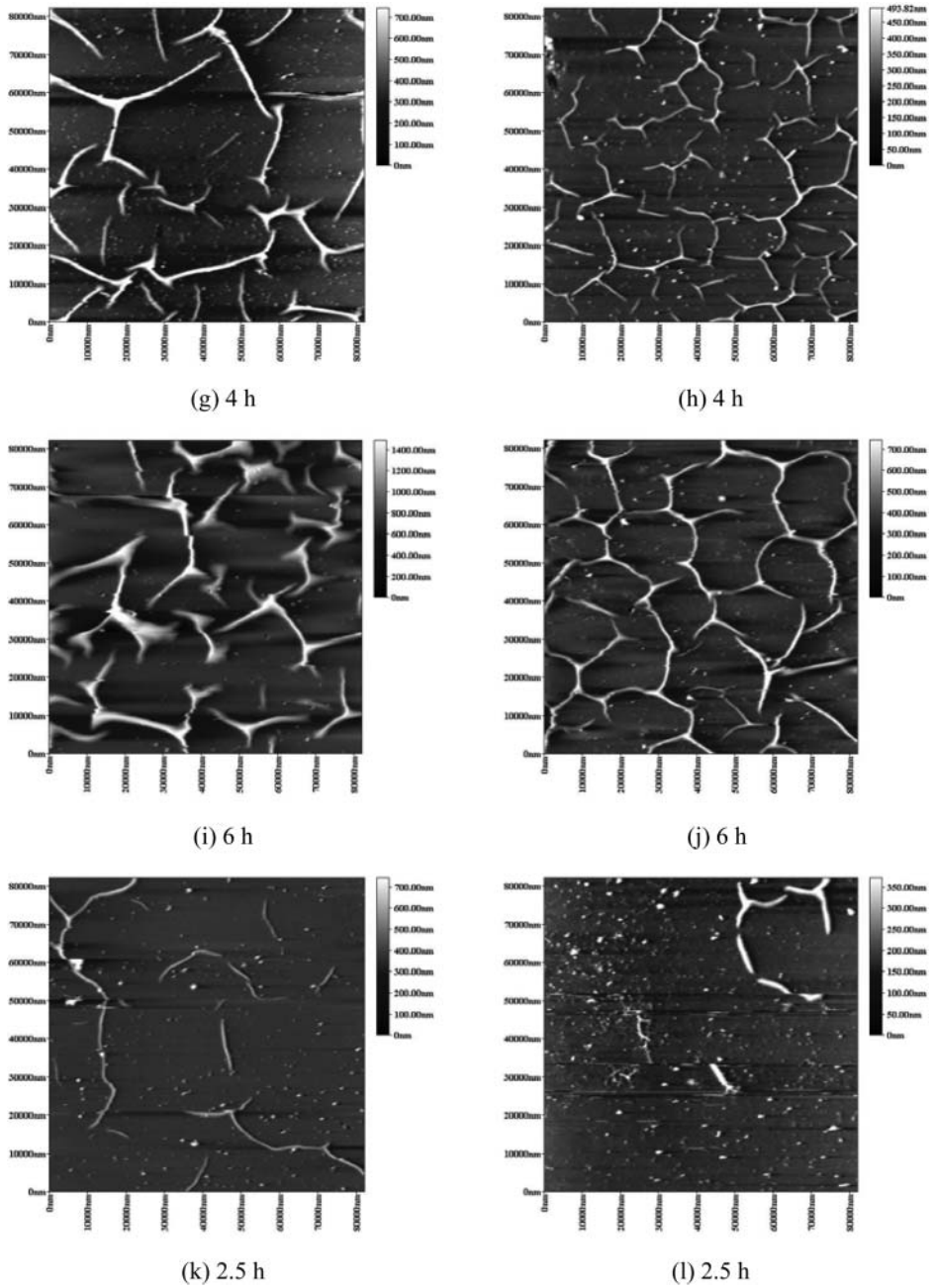


FIG. 5. The AFM images of PPy deposits on the hydrophilic (a, c, e, g, I, and k) versus hydrophobic surfaces of $SiO_2$ substrates (b, d, f, h, j, and l) under different reaction time.

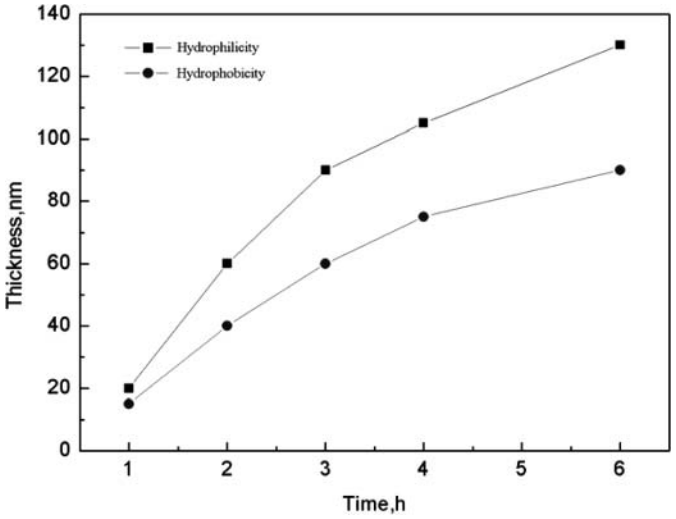


FIG. 6. Plots of thickness (nm) – time (h) of the PPy films grown on various hydrophilic/hydrophobic surfaces of $SiO_2$ substrate.

relationship between the thickness of the film and reaction time, it can be easily concluded that the growing rate for the PPy on hydrophilic surface of $SiO_2$ substrate was much faster. In addition, it was quite an important stage when the reaction time was 2–3 h with the film thickness of 40–70 nm as it was the early stage of the wrinkles forming. The AFM measurements at this stage are shown in Figure 5. It can be concluded from the two images that the smaller separated rod-like unit played an important role in the earlier stage of the wrinkles forming, which further grew bigger and interconnected to form bigger open or closed wrinkles morphology as the reaction time increasing.

Based on the previously mentioned data, it can be concluded the development of the PPy nanoparticles deposition, film growing, and wrinkle morphology forming in general. In the early stage, PPy nanoparticles deposited on not only the hydrophilic surface but also the hydrophobic surfaces of $SiO_2$ substrate to form thin films. Lateral growth then occurred on some parts of the PPy nanoparticles and rod-like morphology showed up. This kind of rod-like PPy branched off or interconnected to form Y- or T-shaped wrinkles as the reaction was in progress, and further formed even bigger wrinkles morphology on a large scale.

It is worthy of noting that the wrinkle morphology on hydrophilic/hydrophobic surface of $SiO_2$ substrates is significantly different from each other, with open Y- or T-shaped wrinkles in the former, but a closed polygon shape in the latter. The reason is ascribed to the difference of the surface energy between the hydrophilic/hydrophobic surface. As the reaction is going on, the continuing growth of PPy nanoparticles was still affected by the surface energy of the hydrophilic/hydrophobic surface of $SiO_2$ substrates because of the memory effect, which was also demonstrated in other research.[15] However, it is still unclear why different open versus closed wrinkles morphology appeared on the two different surface of $SiO_2$ substrates. Further studies are needed to solve this issue.

## CONCLUSION

In conclusion, chemical *in situ* polymerization was a convenient and effective method for preparing PPy conducting film. Wrinkles morphology of open Y- and T-shape on the hydrophilic surface versus closed polygon shape on the hydrophobic surface of $SiO_2$ substrates was observed by means of optical microscope, SEM, and AFM. It was found that different surface energy and the memory effect played an important role in the process of the film growing.

## REFERENCES

1. Zheng, W.; Razal, J.M.; Whitten, P.G.; Ovalle-Robles, R.; Wallace, G.G.; Baughman, R.H.; Spinks, G.M. Artificial muscles based on polypyrrole/carbon nanotube laminates. *Adv. Mater.* **2011**, *23*, 2966–2970.
2. Sevilla, M.; Valle-Vigón, P.; Fuertes, A.B. N-doped polypyrrole-based porous carbons for $CO_2$ capture. *Adv. Funct. Mater.* **2011**, *21*, 2781–2787.
3. Skotheim, T.A.; Reynolds, J.R. *Handbook of Conducting Polymers,* 3rd edn. New York: Taylor & Francis Group, **2007**.
4. Wallace, G.G.; Spinks, G.M.; Teasdale, P.R.; Kane-Maguire, L.A. P. *Conductive Electroactive Polymers: Intelligent Materials Systems, Second Edition*; New York: Taylor & Francis Group, **2003**.
5. Wang, C.Y.; Zheng, W.; Yue, Z.L.; Too, C.O.; Wallace, G.G. Buckled, stretchable polypyrrole electrodes for battery applications. *Adv. Mater.* **2011**, *23*, 3580–3584.
6. Yuan, X.X.; Zeng, X.; Zhang, H.J.; Ma, Z.F.; Wang, C.Y. Improved performance of proton exchange membrane fuel cells with p-toluenesulfonic acid-doped Co-PPy/C as cathode electrocatalyst. *J. Am. Chem. Soc.* **2010**, *132*, 1754–1755.
7. Marchesi, L.F. Q. P.; Simes, F.R.; Pocrifka, L.A.; Pereira, E.C. Investigation of polypyrrole degradation using electrochemical impedance spectroscopy. *J. Phys. Chem. B* **2011**, *115*, 9570–9575.
8. Li, X.G.; Li, A.; Huang, M.R.; Liao, Y.Z.; Lu, Y.G. Efficient and scalable synthesis of pure polypyrrole nanoparticles applicable for advanced nanocomposites and carbon nanoparticles. *J. Phys. Chem. C* **2010**, *114*, 19244–19255.
9. Liao, Y.Z.; Li, X.G.; Kaner, R.B. Facile synthesis of water-dispersible conducting polymer nanospheres. *ACS Nano* **2010**, *4*, 5193–5202.
10. Li, X.G.; Hou, Z.Z.; Huang, M.R. Moloney, M. G. Efficient synthesis of intrinsically conducting polypyrrole nanoparticles containing hydroxy sulfoaniline as key self-stabilized units. *J. Phys. Chem. C* **2009**, *113*, 21586–21595.
11. Zotti, G.; Vercelli, B.; Berlin, A. Gold nanoparticle linking to polypyrrole and polythiophene: Monolayers and multilayers. *Chem. Mater.* **2008**, *20*, 6509–6516.
12. Sutton, S.J.; Vaughan, A.S. On the morphology and growth of electrochemically polymerized polypyrrole. *Polymer* **1995**, *36*, 1849–1857.
13. Shapiro, J.S.; Smith, W.T. A morphological study of polypyrrole films grown on indium-tin oxide conductive glass. *Polymer* **1997**, *38*, 5505–5514.
14. Miles, M.J.; Smith, W.T.; Shapiro, J.S. Morphological investigation by atomic force microscopy and light microscopy of electropolymerised polypyrrole films. *Polymer* **2000**, *41*, 3349–3356.
15. Wang, P.C.; Huang, Z.; MacDiarmid, A.G. Critical dependency of the conductivity of polypyrrole and polyaniline films on the hydrophobicity/hydrophilicity of the substrate surface. *Synth. Met.* **1999**, *101*, 852–853.